Dissolution of a Homogeneous Porous Medium by Surface Reaction

In this paper a mathematical model is used to predict the time behavior of porosity and permeability of a porous medium being dissolved by acid. Experimentally determined reaction kinetics and pore size distribution are used in the model. The acidizing process studied here is of importance in the stimulation of oil well reservoirs. A polynomial expansion method is used to obtain an approximate solution to an infinite hierarchy of moment equations resulting from application of the capillary model. Experimental porosity and permeability measurements using a sintered glass disk dissolved by hydrofluoric acid are in good agreement with predictions from the model.

MARTIN C. GLOVER
and
JAMES A. GUIN
Department of Chemical Engineering
Auburn University
Auburn, Alabama 36830

SCOPE

The first objective of this work was to test experimentally a model proposed by Schechter and Gidley (1969) for describing the evolution in properties of a porous medium under attack by a reactive fluid. The second was to develop a useful, practical method for solving certain equations resulting from application of the model to the physical situation.

The primary impetus for this work is the process occurring in the stimulation of oil wells, wherein an acid is used to dissolve selective portions of the porous reservoir rock, thereby enhancing its permeability to the flow of oil. It would be desirable for engineering design to be able to predict the magnitude of this permeability change as a function of acid treatment conditions. The actual process is made very complex by the heterogeneous nature of natural rock and complicating phenomena including the swelling of clays in the porous matrix, the loosening of fine particles with subsequent clogging of the matrix, and the different reaction rates upon the different minerals present. Before attacking this complex problem in its entirety, it would seem desirable first to be able to adequately model a similar but more idealized process, namely, dissolution of a homogeneous porous medium. Until this has been done, the inclusion of the more complex phenomena noted above seems unwarranted.

The work to date in this area has been summarized by Sinex, Schechter, and Silberberg (1972) who studied the dissolution of bronze porous media. Their work provided a verification of the capillary model for predicting permeability change as a function of porosity change. The present investigation was undertaken to provide a more rigorous test of the model utilizing the pore size distribution and surface reaction kinetics to predict the time dependence of the porosity and permeability.

CONCLUSIONS AND SIGNIFICANCE

Experimental results show that the capillary model is capable of predicting the temporal change of permeability and porosity in a dissolving porous medium using only an independently determined surface reaction rate and initial pore size distribution. No adjustable parameters are used in the model. Numerical results show that an orthogonal polynomial expansion provides a practical and convenient method for solution of the model equations. Because of this favorable verification of the model, work can now be directed toward including the more complex phenomena occurring during dissolution of a naturally occurring heterogeneous porous medium.

This paper is concerned with predicting the changes in permeability and porosity of a porous medium as it is dissolved by a reactive fluid flowing in the interstices. The prediction of these changes is of some importance in the stimulation of oil wells where acids are sometimes pumped into a well to dissolve portions of the rock matrix, thus increasing the permeability and allowing a greater oil production rate (Grubb and Martin, 1963). Today the prediction of well production after acidizing is based largely on experience rather than upon a fundamental design method utilizing reaction kinetics and properties of the porous medium. A design method based upon these latter considerations would be desirable since it would allow calculations to determine optimum acid treating conditions a-priori. While the method explored in this paper has not yet been developed so that it can be used for acidization design purposes, the method is shown to yield good agreement with experiments in a more idealized situation involving a homogeneous porous medium.

One of the earliest investigators who recognized the possible effect of matrix geometry upon acidizing results was Rowan (1959). More recently Schechter and Gidley (1969) proposed a more detailed mathematical model for the acidizing process which included a provision for the surface reaction rate as well as a temporal and spatial dependence of the porous medium geometry. This model has been further developed and experimentally tested by Guin et al. (1969, 1971a, 1971b) and Sinex et al. (1972). These tests have been somewhat limited in that the reaction kinetics and the matrix geometry were not both well defined, or as in some cases, (Guin, 1971b), these two factors did not enter into the calculations. The purpose of this paper is to report a more detailed test of the theory in which both reaction kinetics and matrix geometry are well known. In addition, this work is a more stringent test of the mathematical model than previously made since the time dependence of the permeability and porosity is predicted rather than only the permeability change as a func-

---

Correspondence concerning this paper should be addressed to J. A. Guin. M. C. Glover is with the Exxon Company, Baton Rouge, Louisiana.

tion of porosity.

The mathematical model proposed by Schechter and Gidley (1969) represents the acidizing process by following the changes in a population of cylindrical capillaries as their walls are dissolved by the reactive fluid. These investigators thus replaced the actual porous medium by an idealized model constructed of randomly spaced capillaries having a distribution of cross-sectional areas. By limiting the use of the model to that of predicting only ratios of macroscopic property values rather than the absolute magnitudes of these quantities, they hoped to overcome most of the criticisms commonly leveled at geometric models of this type. As the acid penetrated the idealized porous medium they envisioned that the pore size distribution would be changed by two mechanisms; the first being that whereby all pores would grow larger as their walls were dissolved by surface reaction and the second being a process whereby the wall between two adjacent pores would be completely dissolved away, thus leaving a single larger pore in their stead. This latter mechanism may be referred to as a collision between pores and serves to reduce the total number of pores present while increasing the permeability at an accelerated rate. By considering the effects of these two mechanisms upon the pore population, Schechter and Gidley were able to show that the changes in the pore size distribution $\eta(A, t)$ were described by the following equation:

$$\frac{\partial \eta}{\partial t} + \frac{\partial}{\partial A}(\psi\eta) = \overline{L}\left[\int_0^A \psi(\lambda, t)\, \eta(A-\lambda, t)\, \eta(\lambda, t)\, d\lambda - \int_0^\infty [\psi(\lambda, t) + \psi(A, t)]\, \eta(A, t)\, \eta(\lambda, t)\, d\lambda\right] \quad (1)$$

In Equation (1), $\eta(A, t)\, dA$ represents the number of pores of area $A \rightarrow A + dA$ per unit volume of porous medium, $\overline{L}$ is an average pore length, and $\psi(A, t)$ represents the growth rate of an individual pore due to its wall being eroded by the acid. Schechter and Gidley show that the porosity and permeability of the capillary model are proportional to the first and second moments of the pore size distribution, respectively, so that if the growth rate $\psi(A, t)$ and the initial pore size distribution $\eta(A, 0)$ are known, a prediction of the changes in these two important macroscopic properties results in principle from solving Equation (1). In this investigation independent methods were used for obtaining the pore growth rate and the initial pore size distribution. The growth rate was determined from surface reaction rate data obtained in laminar flow experiments using Pyrex glass tubes. Thus the complex porous medium geometry did not enter into the calculations for pore growth rate. The initial pore size distribution for the model calculations was obtained from the experimental study of Felch and Shuck (1971), who determined a capillary pore size distribution for coarse fritted glass disks by utilizing the fact that the flux of solute diffusing through a pore depends upon its cross-sectional area.

REACTION KINETICS

The reaction system used in this study was composed of Pyrex 7740 glass and hydrofluoric acid. This system bears some similarity to the sandstone-HF system encountered in oil well acidizing in that the primary constituent of both sandstone and Pyrex glass is SiO_2. One difference is that sandstone is composed of α-quartz, a crystalline form, while Pyrex glass is amorphous, and for this reason we would not expect the reaction rate of these two solids with HF to be exactly equal.

In order to determine the growth rate $\psi(A, t)$ appearing in Equation (1), it is necessary to determine the average reaction rate over the surface of a pore. For a cylindrical pore having a perimeter Γ, a length $\overline{L}$, and undergoing a first-order surface reaction, the average reaction rate is defined as

$$R_{av} = \frac{1}{\overline{L}} \int_0^{\overline{L}} k c_s\, dx \quad (2)$$

where c_s indicates the concentration of acid at the surface. Sinex (1972) shows that the function $\psi(A, t)$ is given in terms of this average surface reaction rate by

$$\psi(A, t) = \frac{2\sqrt{\pi}\, \gamma R_{av}}{\rho_s} A^{1/2} \quad (3)$$

Thus, if R_{av} is independent of the pore area, the growth rate will be proportional to the square root of the pore area. We shall see that this situation prevails with the Pyrex glass-HF surface reaction.

The stoichiometry of the reaction between Pyrex 7740 glass and HF is rather complex as Pyrex is a mixture of the following compounds: SiO_2, 81%; Na_2O, 4%; Al_2O_3, 2%; and B_2O_3, 13% (Bolz, 1970). The first three compounds react in only one way with HF.

$$6HF + SiO_2 \rightarrow H_2SiF_6 + 2H_2O$$

$$2HF + Na_2O \rightarrow 2NaF + H_2O$$

$$6HF + Al_2O_3 \rightarrow 2AlF_3 + 3H_2O$$

Depending upon reaction conditions, boron trioxide and HF may react to form one or more of three different compounds.

$$4HF + B_2O_3 + H_2O \rightarrow 2H_3BO_2F_2$$

$$6HF + B_2O_3 \rightarrow 2HBF_3OH + H_2O$$

$$8HF + B_2O_3 \rightarrow 2HBF_4 + 3H_2O$$

One quantity that is needed for the complete analysis of the reaction system is the stoichiometric coefficient, γ:

$$\gamma = \frac{\text{mass Pyrex 7740 reacted}}{\text{mass HF expended}}$$

Two methods were used to determine γ for this system. The first involved the use of the composition of Pyrex 7740 and the balanced equations for the reaction of each component with HF. This assumes that Pyrex 7740 is of fairly homogeneous composition and that HF does not selectively attack the more reactive components. Since B_2O_3 and HF react in three different proportions, this method results in a range of values for γ of 0.541 to 0.597 g Pyrex 7740/g HF. The second method was a direct experimental determination in which Pyrex tubes were placed in a solution containing a known amount of HF and allowed to react until equilibrium was attained. In this way a value of $\gamma =$ 0.60 g Pyrex/g HF was obtained which is quite consistent with the range of values obtained from consideration of the stoichiometric equations. This experimentally determined value was used in the remaining calculations in this paper.

Because the kinetics of fluid-solid surface reactions can be masked by mass transfer effects, it is useful to obtain kinetic data in a system wherein these effects can be accounted for. Such a system has been discussed by Williams et al. (1970) who showed that the average surface reaction rate in a circular tube was given in the case of a first-order reaction by

$$R^* = 4PL^* \left[1 + \sum_{n=1}^{\infty} \beta_n \frac{3}{n+3} \left(\frac{\Gamma(1/3)P}{3} \right)^n \left(\frac{9L^*}{2} \right)^{n/3} \right] \tag{4}$$

where P is a dimensionless surface reaction rate parameter, L^* is a dimensionless length, and R^* is a dimensionless reaction rate (see Notation). In the experiments conducted here, HF solutions at various concentrations and temperatures were allowed to flow laminarly through 3.1 mm (1/8 in.) I.D. precision bore tubing composed of Pyrex 7740 glass. Using the weight loss of the glass tube over a short time interval and the stoichiometric ratio of $\gamma = 0.60$ g of glass/g of acid, the average reaction rate defined in Equation (2) was determined. The surface reaction rate constant k could then be found from Equation (4) by an iterative procedure reported by Glover (1972). Since the rate constant k was found to be the same at various acid concentrations, the assumption of a first-order reaction was justified. By performing experiments at several temperatures the Arrhenius plot shown in Figure 1 was constructed. The straight line provided further evidence that the assumption of a first-order reaction was valid. Using Figure 1 the reaction rate for HF and Pyrex glass was determined to have an activation energy of 9.75 kcal/g mole with frequency factor $k_0 = 1.70 \times 10^2$ cm/s. It is notable that the first term in the infinite series of Equation (4) was never less than −0.02, thus indicating that diffusional limitations were not significant in the surface reaction experiments carried out here. That is, the reaction was essentially kinetically controlled. The reaction rate constant determined in these experiments now can be used to deduce the pore growth rate appearing in Equation (3) as described below.

The porous media used in the acidizing experiments were fritted glass disks also composed of Pyrex 7740 glass and designated as type 40C by the Corning Glass Company (Cat. No. 31000). A pore size distribution for these disks was determined by Felch and Shuck as

$$\eta(A, 0) = \text{constant} \times A^{42.9} e^{-0.0431A} \tag{5}$$

where A is the pore area in sq. microns. This experimentally determined pore size distribution was used in the calculations as an initial condition for Equation (1). This distribution, pictured in Figure 2 at $\tau = 0$, predicts an average pore area of 1020 square microns which is quite consistent with the average nominal pore diameter of 40 microns given by Corning for the type 40C disk. Since the fritted glass disks are manufactured rather than naturally occurring, we do not expect significant variations in the pore size distribution among different disks. This was borne out by performing experiments with several disks. In order to determine the growth rate of a pore through Equation (3) it is necessary to determine an expression for R_{av} as it actually occurs in the porous matrix. To do this, we apply Equation (4) to a typical pore of area A in the capillary model. Under the experimental conditions reported by Glover (1972), the lowest fluid velocity through the pores was approximately 0.16 cm/s. Using this information together with the values $\overline{L} = 0.30$ cm, $D = 10^{-5}$ cm²/s, $A = 1000\ \mu^2$, and $k = 1.26 \times 10^{-5}$ cm/s, we find that the absolute value of the first term of the series in Equation (4) is less than 0.01, indicating a kinetically controlled surface reaction in the porous medium. Since the series in Equation (4) alternates, this is the maximum error incurred by neglecting all terms in the sum. Accepting this small error, we may write the average reaction rate in a pore as $R_{av} = kc_0$ where c_0 is the inlet acid concentration. Using this information in Equation (3) the growth rate of a circular pore in the capillary model is found to be

$$\psi(A, t) = \frac{2\sqrt{\pi}\,\gamma k c_0}{\rho_s} A^{1/2} \tag{6}$$

Using typical pore dimensions and noting that R^* equals the fraction of acid reacted, Equation (4) also indicates that less than 1% of the acid reacts in the porous medium,

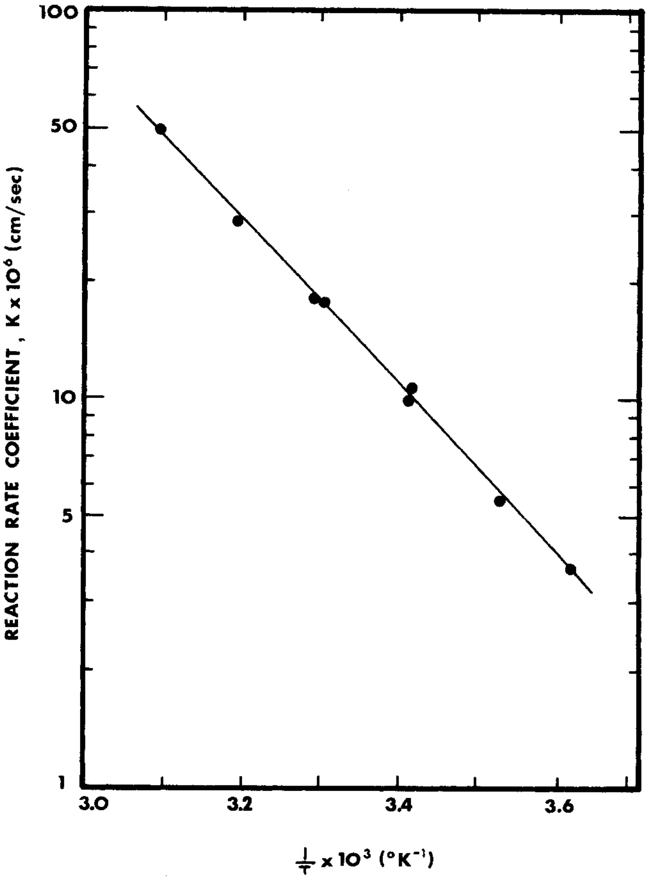

Fig. 1. Arrhenius plot for the surface reaction of Pyrex 7740 glass and hydrofluoric acid.

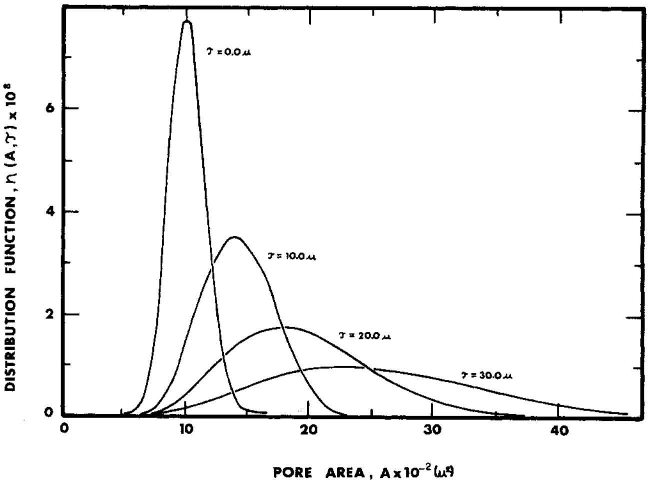

Fig. 2. Calculated changes in pore size distribution during matrix acidization.

allowing us to neglect the spatial dependence in the changing porous medium properties. The problem of predicting the permeability and porosity changes in the fritted glass disks as they are dissolved by HF is now reduced to solving Equation (1) with the growth rate of Equation (6) and the initial pore size distribution given in Equation (5). A comparison with experiment can then be made.

SOLUTION OF THE EVOLUTION EQUATION

Solving a nonlinear integrodifferential equation such as Equation (1) is not straightforward. This motivated Sinex et al. to simulate numerically the behavior of 1000 pores on a digital computer rather than to solve Equation (1) directly. This Monte Carlo simulation has the advantage of numerical stability; however, it has the disadvantages of requiring large computer time and storage and the inherent statistical scatter in the results. That is, the method is not completely deterministic since only 1000 pores can be drawn randomly from a given population density such as that in Equation (5). Because of these disadvantages, a different method of calculation was chosen here. The final results are found to support the Monte Carlo calculations of Sinex.

Since the primary quantities of interest are the first and second moments of the distribution function, it is convenient to multiply Equation (1) by $A^j dA$ and integrate from zero to infinity obtaining

$$\frac{\partial M_0}{\partial \tau} = -\bar{L} M_0 I_0 \tag{7}$$

$$\frac{\partial M_j}{\partial \tau} = j I_{j-1} + \bar{L} \sum_{s=1}^{j-1} \binom{j}{s} M_s I_{j-s} \quad j = 1, 2, \ldots \tag{8}$$

Here the jth moment of the pore size distribution is defined by

$$M_j = \int_0^\infty A^j \eta(A, \tau)\, dA \tag{9}$$

and the integrals I_j are given by

$$I_j = \int_0^\infty A^j \psi(A, \tau)\, \eta(A, \tau)\, dA \tag{10}$$

In Equations (7) and (8) we have introduced for time the independent variable $\tau = \int_0^t f(t)dt$ where $f(t)$ is found by writing Equation (6) as $\psi = f(t)A^{1/2}$. Note that in this case τ has dimensions of length even though it measures the progress of the acidization in time. Hence, we have called τ a reduced time variable in this work. The system represented by Equations (7) and (8) has practical value only if the I_j in Equation (10) can be calculated or approximated using a finite number of the moments M_j. In this situation the infinite hierarchy can be closed and Equations (7) and (8) solved for M_1 and M_2 (proportional to the porosity and permeability, respectively). A method for doing this has been explored by Hulburt and Akiyama (1969) and Holway (1967). This procedure consists of expanding the distribution function in a series of Laguerre polynomials which are orthogonal with respect to a time varying weight function.

For the calculations in this study, we expand $\eta(A, \tau)$ as

$$\eta(z, \tau) = z^\alpha e^{-z} \sum_{v=0}^{N} c_v^\alpha L_v^\alpha(z) \tag{11}$$

The new independent variable z is given by $z = (\alpha - 1)A/a$ and the L_v^α are generalized Laguerre polynomials defined by the relation

$$L_n^\alpha(z) = \frac{e^z z^{-\alpha}}{n!} \frac{d^n}{dz^n} (e^{-z} z^{\alpha+n})$$

These polynomials possess the useful orthogonality property given by

$$\int_0^\infty z^\alpha e^{-z} L_m^\alpha(z) L_n^\alpha(z) dz = \begin{Bmatrix} 0 & ; & m \neq n \\ \dfrac{\Gamma(n+\alpha+1)}{n!}; & & m = n \end{Bmatrix} \tag{12}$$

The use of Equations (11) and (12) shows that the coefficients c_v^α can be calculated from a finite number of moments of the distribution function according to

$$c_v^\alpha = \frac{v!}{\Gamma(v+\alpha+1)} \sum_{k=0}^{v} \frac{(-1)^k \binom{v}{k} \left(\frac{\alpha+1}{a}\right)^{k+1} M_k}{\Gamma(k+\alpha+1)} \tag{13}$$

In order to obtain a rapidly convergent expansion in Equation (11), the time dependent parameters α and a are chosen to cause the coefficients c_1^α and c_2^α to vanish. Thus, Equation (13) shows that to ensure this desirable behavior we must choose

$$\alpha = \frac{M_1^2}{M_0 M_2 - M_1^2} - 1 \tag{14}$$

$$a = M_1/M_0 \tag{15}$$

The integrals I_j in Equation (10) can now be calculated conveniently by expanding the term $A^j\psi(A,\tau)$ in a Laguerre polynomial series and using the orthogonality relation of Equation (12). For the growth function in Equation (6) this process yields

$$I_j = \left(\frac{a}{\alpha+1}\right)^{3/2} \sum_{n=0}^{N} c_n^\alpha D_n^\alpha \frac{\Gamma(n+\alpha+1)}{n!} \tag{16}$$

where the D_n^α are given by

$$D_n^\alpha = \sum_{m=0}^{n} \frac{(-1)^m \binom{n}{m} \Gamma(m+\alpha+j+3/2)}{\Gamma(m+\alpha+1)} \tag{17}$$

The calculation scheme for solving Equations (7) and (8) may now be summarized. An order of approximation N in Equation (11) is decided upon and the coefficients c_v^α are then found from the first N moments of the distribution function. A numerical integration method may then be used to solve the N equations represented by Equations (7) and (8) with the I_j being evaluated by Equation (16). Since the system of N equations is now closed, their solution presents no additional difficulty.

The success of the calculation method presented above depends upon how well the actual distribution function is approximated by Equation (11). This approximation becomes better in a mean square sense as the number of terms N in the expansion is increased. Thus, one way of empirically checking the accuracy of the calculations is to compare the solutions for various orders of approximation. Performing this test, we found that there was virtually no difference in the solutions with $N = 3$ and $N = 4$, and therefore the series in Equation (11) was truncated at $N = 4$. An additional check was performed using the exact solution to Equations (7) and

(8) obtainable when the terms multiplying $\overline{L}$ are equated to zero. Physically this approximation corresponds to neglecting pore collisions in the model of Schechter and Gidley (1969). The Laguerre expansion with $N = 4$ was in excellent agreement with this exact solution (Glover, 1972). A final check on our calculations was made by comparison with the Monte Carlo calculation of Sinex et al. (1972) as is shown in Figure 3. This comparison was made utilizing two different initial pore size distributions, *namely*, a gamma distribution and a square wave distribution, both having an initial porosity of 0.35. The broad band indicates the range of results obtained by Sinex. This agreement may be taken as further evidence of the validity of both the polynomial expansion and the simulation methods.

COMPARISON WITH EXPERIMENT

In the porous media experiments, four Pyrex 7740 sintered glass disks were acidized with a dilute aqueous HF solution with the pressure drop across the disk being monitored continuously. From this data it was possible using Darcy's law to compute the permeability ratio as the acidizing process proceeded. Experimental data from these experiments is compared with the theoretical predictions of the capillaric model in Figures 4 and 5. The solid lines pictured in Figures 4 and 5 are theoretical predictions obtained by solving Equations (7) and (8) with the growth function of Equation (6) using the polynomial expansion method outlined above. The agreement depicted here is considered to be quite good in view of the fact that the theory contains no adjustable parameters for curve fitting. The two theoretical curves were predicted using only the rate constant determined in the re-

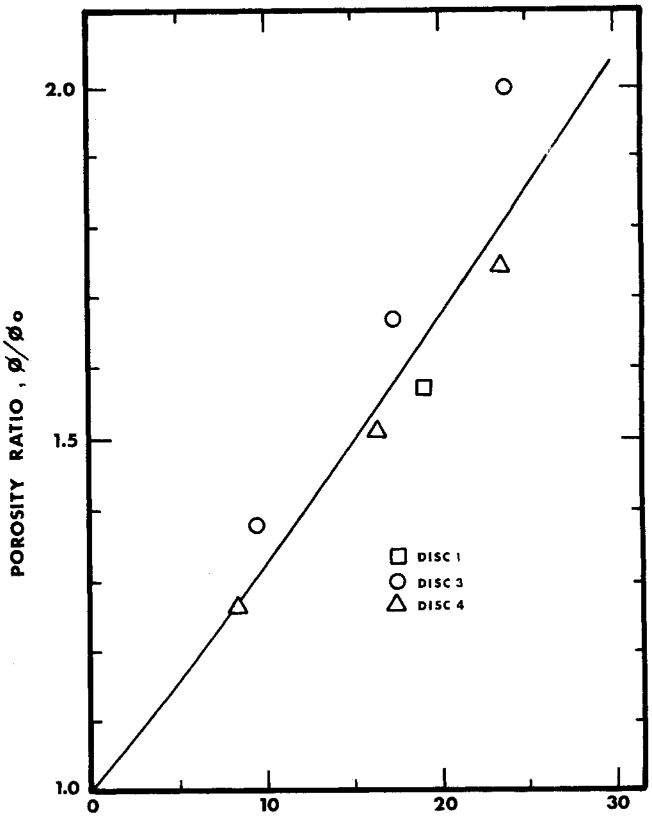

Fig. 4. Comparison of experimental and predicted porosity improvement.

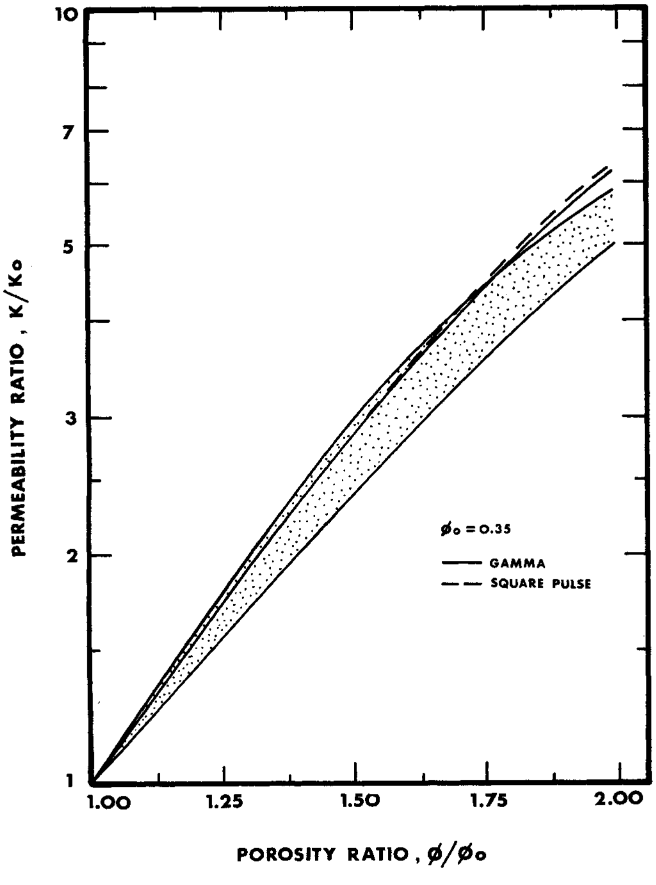

Fig. 3. A comparison between solutions obtained by a numerical simulation and a Laguerre polynomial expansion.

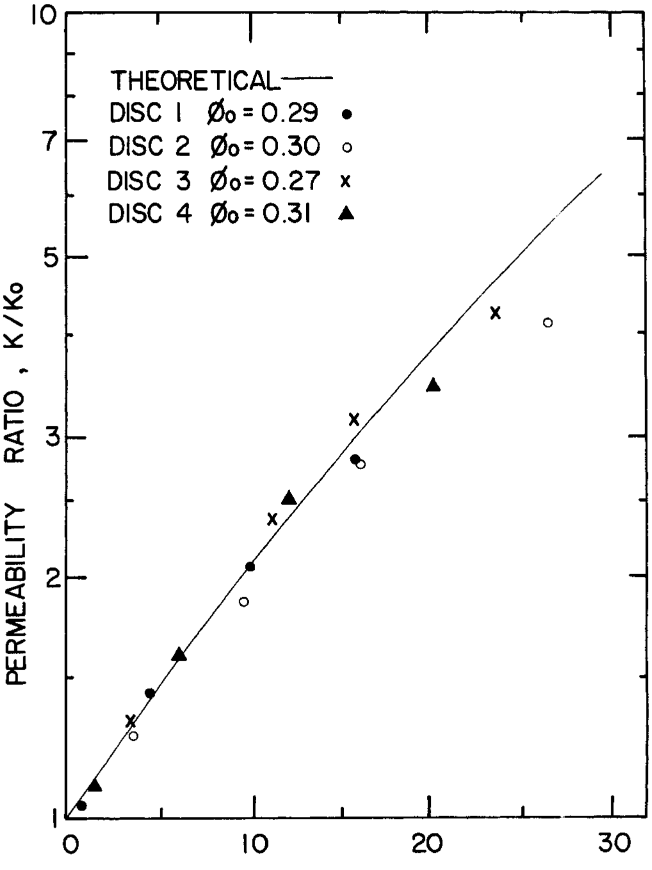

Fig. 5. Comparison of experimental and predicted permeability improvement.

action kinetics experiments and the initial pore size distribution in Equation 5. Figure 4 indicates the porosity change of three disks as a function of time from the start of the acidizing process. Recall that for the growth function of Equation (6), the variable $\tau = 2\sqrt{\pi}\,\gamma\,k\,c_0\,t/\rho_s$. The fact that the data for disk 3 are consistently above the theoretical curve in Figure 4 may be due to experimental error in determination of the initial porosity. Since all values of the porosity ratio are referred to this initial value, such an error would have the effect of raising each of the points in Figure 4. Some support for this hypothesis is gained by noting that the initial porosity measured for disk 3 was 0.27, the lowest value of the four disks acidized. Since these manufactured disks should be relatively consistent in initial properties, consideration of the initial porosities for the other three disks (see Figure 5) indicates that the value of 0.27 might be low. An adjustment of the initial porosity of disk 3 to, say 0.30, would cause the points depicted for disk 3 to agree better with prediction. No porosity measurements were made on disk 2 as it was not removed from the acidizing cell until it had become unconsolidated.

The time variation of permeability for all disks acidized is shown in Figure 5. Consideration of Equation (1) shows that there would be an effect of initial porosity on the location of the theoretical curve in Figure 5; however, this effect was found to be so small that a single theoretical curve accurately represented the predicted permeability change for all the disks. Some disk unconsolidation with subsequent clogging of the pores may be occurring in the final stages of the process, causing the measured permeability values to lie slightly below the predicted value.

An idea of how the pore size distribution $\eta(A,\tau)$ changes during the acidizing process may be obtained directly from Equation (11) and is presented in Figure 2. It can be seen that the average pore area more than doubles and that the relatively narrow initial distribution (characteristic of sintered disks) becomes much more disperse with some relatively large pores being formed. These larger pores are primarily the result of the collision process discussed in more detail by Guin and Schechter (1971a). If it were not for this mechanism, the largest pores in Figure 3 would have an area less than $3000\mu^2$ at $\tau = 30\mu$.

CONCLUSIONS

This work provides verification for a mathematical model of matrix acidizing in which both experimentally determined reaction kinetics and initial pore size distribution are used. Comparison with experiment has shown the capillary model to yield a valid prediction of the porosity and permeability improvement obtained by acidizing. A polynomial expansion method has been shown to be a useful method for solution of the equations resulting from application of the capillary model.

The surface reaction between dilute aqueous HF solutions and Pyrex 7740 glass (81% SiO_2) was found to be first order and to fit the Arrhenius model with an activation energy of 9.75 kcal/g mole and a frequency factor of 1.70×10^2 cm/s. The reaction was kinetically controlled under the experimental conditions used here.

ACKNOWLEDGMENT

M. C. Glover wishes to express gratitude to Texaco, Incorporated for fellowship support during this work. J. A. Guin wishes to acknowledge support from the Auburn University Engineering Experiment Station, Auburn University Grant-in-Aid 70-61 and NSF Grant GK-37460.

NOTATION

A = cross-sectional area of a pore
c = acid concentration
D = molecular diffusivity of acid
k = first-order surface reaction rate parameter
L^* = dimensionless axial length, $\bar{L}D/2\bar{V}R^2$ for a circular pore
$L_n^{\alpha}(z)$ = generalized Laguerre polynomial
$\bar{L}$ = mean pore length
M_j = moment of pore size distribution function
P = dimensionless surface reaction rate parameter, kR/D for a circular pore
R = pore radius
R^* = dimensionless reaction rate, $2R_{av}\bar{L}/c_0\bar{V}R$ for a circular pore
R_{av} = average surface reaction rate in a pore
t = time
$\binom{m}{n}$ = binomial coefficient, $\frac{m!}{(m-n)!\,n!}$

Greek Letters

ϕ = porosity
η = pore size distribution function
ρ_s = solid density
γ = mass of solid dissolved/mass of HF expended
ψ = growth rate for a single pore
τ = reduced time variable

LITERATURE CITED

Bolz, R. E., and G. L. Tuve, (eds.), "Handbook of Tables for Applied Engineering Science," p. 123, Chemical Rubber Co., Cleveland, Ohio (1970).

Felch, D. E., and F. O. Shuck, "Determination of Pore Size Distribution in Porous Materials," *Ind. Eng. Chem. Fundamentals,* 10, 299 (1971).

Glover, M. C., "Surface Reactions in Porous Media," M.S. thesis, Auburn Univ., Alabama (1972).

Grubb, W. E., and F. G. Martin, "A Guide to Chemical Well Treatments," *Petrol Eng.* 100 (August, 1963).

Guin, J. A., "Chemically Induced Changes in Porous Media," Ph.D. dissertation, Univ. Texas, Austin, Texas (1969).

———., and R. S. Schechter, "Matrix Acidization with Highly Reactive Acids," *Soc. Petrol. Eng. J.,* 11, 390 (1971a).

———., I. H. Silberberg, and R. S. Schechter, "Chemically Induced Changes in Porous Media," *Ind. Eng. Chem. Fundamentals,* 10, 50 (1971b).

Holway, L. H., "Time Varying Weight Functions and the Convergence of Polynomial Expansions," *Phys. Fluids,* **10,** 35 (1967).

Hulburt, H. M., and T. Akiyama, "Liouville Equations for Agglomeration and Dispersion Processes," *Ind. Eng. Chem. Fundamentals,* 8, 319 (1969).

Rowan, G., "Theory of Acid Treatment of Limestone Formations," *J. Inst. Petrol,* 45, 321 (1959).

Schechter, R. S., and J. L. Gidley, "The Change in Pore Size Distribution From Surface Reactions in Porous Media," *AIChE J.,* 15, 339 (1969).

Sinex, W. E., R. S. Schechter, and I. H. Silberberg, "Dissolution of a Porous Matrix by a Slowly Reacting Acid," *Ind. Eng. Chem. Fundamentals,* 11, 205 (1972).

Williams, B. B., J. L. Gidley, J. A. Guin, and R. S. Schechter, "Characterization of Heterogeneous Fluid—Solid Reactions—The HCl—$CaCO_3$ Reaction," *Ind. Eng. Chem. Fundamentals,* 9, 589 (1970).

Manuscript received April 9, 1973; revision received and accepted July 9, 1973.